Talanta 142 (2015) 57–63 | Post-print

Portable gliadin-immunochip for contamination control on the food production chain

Maria Serena Chiriacò[a*], *Francesco de Feo*[a], *Elisabetta Primiceri*[a], *Anna Grazia Monteduro*[a], *Giuseppe Egidio de Benedetto*[b], *Antonio Pennetta*[b], *Ross Rinaldi*[a] *and Giuseppe Maruccio*[a*]

[a] NNL Istituto Nanoscienze - CNR and Dipartimento di Matematica e Fisica "Ennio De Giorgi"- via per Arnesano, 73100 Lecce
[b] Laboratorio di spettrometria di massa analitica ed isotopica, Dipartimento di beni culturali, Università del Salento, 73100 Lecce
* Corresponding authors: serena.chiriaco@unisalento.it , giuseppe.maruccio@unisalento.it

DOI: 10.1016/j.talanta.2015.04.040

Abstract

Celiac Disease (CD) is one of the most common digestive disorders caused by an abnormal immune reaction to gluten. So far there are no available therapies, the only solution is a strict gluten-free diet, which however could be very challenging as gluten can be hidden in many food products. Furthermore an additional problem is related to cross-contamination of nominal gluten-free foods with gluten-based ones during manufacturing. Here we propose a lab on chip platform as a powerful tool to help food manufacturers to evaluate the real amount of gluten in their products by an accurate *in-situ* control of the production chain and maybe to specify the real gluten content in packages labelling. Our portable gliadin-immunochips, based on an electrochemical impedance spectroscopy transduction method, were first calibrated and then validated for both liquid and solid food matrixes by analysing different beers and flours. The high specificity of our assay was also demonstrated by performing control experiments on rice and potatoes flours containing prolamin-like proteins. We achieved limit of quantification of 1.5 ppm for gliadin that is 20 times lower than the worldwide limit established for gluten-free food while the method of analysis is faster and cheaper than currently employed ELISA-based methods. Moreover our results on food samples were validated through a mass spectrometry standard analysis.

Keywords
Lab on chip, Celiac disease, Gliadin-Immunochip, Electrochemical impedance spectroscopy, microfluidics, on-chip contamination control.

1. Introduction

General aspects of Celiac Disease

Celiac Disease (CD), also known as gluten-sensitive enteropathy [1], is an autoimmune-mediated [2, 3] systemic disorder [4], based on a genetic predisposition [5]. Once it was considered to be a rare childhood condition, but now it is recognized to be a very common pathology. It affects around 1% of worldwide population [6, 7] and it occurs throughout the entire lifespan. In genetically susceptible individuals, gliadin fragments in the intestinal lumen induce a signalling cascade, causing the autoimmune system activation and it results in a chronic inflammation of the small intestine mucosa with villous atrophy and consequently malabsorption of nutrients. Due to its unspecific symptoms [8-10], CD may incur in an incorrect initial diagnosis for irritable bowel syndrome (IBS), colitis, Crohn disease, gastroenteritis of infective nature. Although a large number of medications are available for symptom relief, the only CD effective treatment is life-long abstinence of gluten ingestion. Such uncomfortable condition is made even more critical by difficulties to keep a gluten-free diet since gluten can be hidden in many foods and other consumables (medications, flavourings, candies, sauces). Minimum tolerable amount of gluten in the diet is still controversial [11][12]. In this respect, designations like “low gluten”, “gluten-reduced” or “gluten-free” foods might not help and create confusion among consumers because of disagreements about the cereal origin and gluten amount that a “gluten-free” food can contain [13]. In 2008 FAO/WHO food standard programme, gluten content levels from 20 up to 100 ppm were proposed [14] to define a gluten free food.

Current methods for Gliadin detection

Gliadin belongs to the prolamin family rich in proline and glutamine [15], which represents the alcohol-soluble fraction of gluten, and it can be classified on the basis of their electrophoretic mobility (α/β-, γ-, ω-gliadins in order of decreasing mobility) [16] but all of them have in common repetitive portion,

upstream the group-specific aminoacidic sequence rich in proline and glutamine. Presently, for evaluating the gluten content of food two different methods, both based on a sandwich enzyme-linked immunosorbent assay, are endorsed by a variety of organizations, including the Codex Alimentarius Commission and the Association of Analytical Communities (AOAC) [17]. For instance ω-gliadin ELISA [18], employs monoclonal antibodies recognizing the ω-gliadin fraction of wheat in both heated and unheated food, but this method greatly underestimates barley hordein content in barley-contaminated foods [13] with a limit of quantification of 150 ppm of gluten, assuming a gliadin-to-glutenin ratio of 1:1 [19]. On the other hand, standard R5 ELISA exploits the R5 monoclonal antibody directed against the potentially toxic celiac epitope QQPFP (glutamine-glutamine-proline-phenylalanine-proline) reaching a limit of detection (LOD) of 1.5 ppm gliadin, corresponding to 3 ppm gluten and a limit of quantification of 2.5 ppm gliadin, corresponding to 5 ppm gluten in heated and unheated food. A further improvement of the R5 ELISA test requires formulation of new cocktail solutions for extracting gliadin from foods, including enzymes for digestion of prolamins [20], or the introduction of competitive assays to reach lower limits of detection but this would result in a significant increase of test duration and cost. Molecular biology techniques were also used to detect wheat DNA in food by developing a quantitative real-time PCR system with sensitivity similar to that of standard ELISA tests[21] .

Technological improvements for gliadin sensors

Recently, Peres et al. have developed an electronic tongue-device able to classify spiked samples of “gluten-free”, “low gluten content” or “gluten-containing” foods on the basis of a potentiometric sensor array reaching a sensitivity of 1–2 mg/kg (corresponding to 1-2 ppm) [22]. In 2012, Chu et al. have proposed a label-free QCM gliadin immunosensor using anti-gliadin antibodies immobilized on gold nanoparticles and reporting a measurable frequency change when 1 ppm gliadin was bound from food samples [23]. Here we report a new approach for on-chip detection of gliadin which is based on the same

interaction but combines an electrochemical immunosensor with a microfluidic module for the delivery of solutions on the sensing areas functionalized with anti-gliadin antibodies.

The transduction method employed in this work is based on Electrochemical Impedance Spectroscopy (EIS), which, since its first applications in biological studies [24-26] , has risen as a powerful technique for the development of lab-on-chip devices. EIS is a method suitable for both cellular [24, 27] and molecular [28] analysis and it can be applied to the high throughput screening of drugs and toxic compounds on cell lines [29, 30], cell-based sensors towards artificial taste organs [28] and the study of the dynamics of biorecognition events between molecules [31-34]. To fully exploit this promising technique we developed an impedimetric platform to detect gliadin from food samples.

Despite the large spreading of the disease, there is lack of portable tests for *in-situ* analysis of foodstuffs and to our knowledge our platform is the first optimized example of a portable impedance device for gliadin detection. One of the rare examples already reported in literature regarding platforms for *in-situ* detection of toxic fraction of gluten was developed by Mairal et al. in 2009. They realized a 5 channel-microfluorimeter device for fluoroimmunoassays with an integrated system including a LED (λ = 477 nm) and an amplified detector, which allowed to reach a LOD for gliadin of 4,1 ng/ml from foodstuff [35].

Our device was first calibrated with spiked samples of gliadin in ethanol/PBS solutions reaching a limit of quantification (LOQ) of 0.5 μg/ml of gliadin, corresponding to a concentration of 0.5 ppm gliadin and 1 ppm gluten, and a calculated limit of detection (LOD) of 0.2 ppm. For proof of concept, our biochip was then used for the detection of gluten in beer and flour samples. Our results demonstrate the possibility to easily discriminate between gluten-free and gluten-containing products without being heavily affected from matrix effects. The achieved limit of detection is very low and well below the values worldwide approved guidelines to label a gluten-free food. To validate our on-chip analysis of food samples we have performed also a Mass spectrometry analysis quantification.

Furthermore our integrated microfluidic platform allows to exploit the advantages of flow immunoassays as quantitative results, speed, reduced sample handling and costs. There is no need for fluorescent tagging of reagents, no PCR amplification and no complex instrumentation or skilled operators are necessary. Our gliadin detection biochips represent a robust, portable platform for a fast and low cost analysis of gliadin levels in foods, which is very suitable for use in food factories producing both gluten-based and gluten-free products since it can allow to test, at the same time, different batches of products for their gliadin content or to check foodstuffs for cross contamination.

2. Materials and methods

2.1 Chip Fabrication and functionalization

The gliadin detection biochip reported here integrates a microfluidic module with four separate sensing areas each one containing four transducer arrays made of 8 gold interdigited microelectrodes. Each couple of IDEs covers an area of 0.5 x 0.7 mm, thus containing 26 metal fingers with connectors to pad.The microelectrodes (10 μm width and spaced) were fabricated on silicon substrates by optical lithography and lift-off (Figure 1a), while the microfluidic PDMS module was realized by replica molding with 20 μL chambers (5 x 1 mm in diameter and height) connected with inlet and outlet microchannels for fluids handling (Figure 1b). Biosensing capability was achieved by means of a specific functionalization of the gold microelectrodes (Figure 1c) using reagents from Sigma Aldrich at the maximum degree of purity. In particular the first step was an overnight deposition of a mixed SAM of 11-mercaptoundecanoic acid (MUA) and 2-mercaptoethanol (2-ME) in a ratio of 1:5 (0.2 mM of MUA and 1mM of 2-ME) followed by activation of the COOH groups by means of an incubation with N-hydroxysuccinimide (NHS) and N-ethyl-N'-(3-dimethylaminopropyl) carbodiimide hydrochloride (EDC) in milliQ water to form reactive N-hydroxysuccinimide esters [36, 37]. Electrodes were then incubated consecutively in solutions with (i) protein A (50 mg/ml), which will allow an oriented immobilization of antibodies through their constant

portion, (ii) ethanolamine (1 M) to deactivate excess esters and (iii) BSA (Bovine Serum Albumin, 5 mg/ml) solution to saturate the electrode unbounded sites and make homogeneous the new surface that will hold the antibodies. The sensing electrodes were finally functionalized with anti-gliadin (wheat) antibody (1µg/ml) from Sigma Aldrich reacting positively with gliadin antigens from wheat (heated and unheated), rye, soy, barley and weakly from oats. Two kinds of negative controls were also set up: one contained a unspecific antibody (Anti-Listeria monoclonal antibody from Santa Cruz Biotech) which was tested against the same foodstuffs employed for experiments; the other one was functionalized with Anti-Gliadin antibodies and it was also tested for recognition of other "prolamins-like proteins" from rice [38] and potatoes [39]. All the steps of functionalization of the electrodes were performed delivering solutions directly into the microfluidic module by using syringe pumps (from Ugo Basile model KDS 270) through the central inlet hole with a flow rate of 10 µl/min to ensure a controllable and reproducible deposition of the functionalization layers in all four chambers at the same time. When a different functionalization of the chambers is required, as in the case of different antibody deposition for control experiments, that could be done by injecting solution from the peripheral hole and controlling the flow so that chambers are filled with the required reagents. The injection of the sample to be analysed instead, can be performed by using a micropipette (or an insulin syringe) to fill the microchambers by the central inlet hole with around 90 µl of extract (each chamber has 20 µl volume).

2.2 Electrochemical measurements

Impedance measurements were performed with a potentiostat (Autolab PGSTAT30) in the frequency range between 0.1 and 10^5 Hz in presence of a potassium hexacyanoferrate (II/III) $K_3[Fe(CN)_6]/K_4[Fe(CN)_6]$ (1:1) solution (Sigma Aldrich) at a final concentration of 10 mM in PBS delivered in the chambers of the device through the microfluidic module (Figure 1b). A sinusoidal 15 mV AC voltage was applied. Bare electrodes (without molecules adhering on them) show a low impedance

since redox reactions, enhanced by the redox couple in the medium, can easily take place, allowing electron transfer from the species in the solution to the electrodes. As subsequent molecular layers are deposited onto the electrode surface (during functionalization or detection phases), the electron transfer process is hindered and this results in an increase of the measured impedance. Faradaic impedance spectroscopy is thus very effective for detecting biorecognition events on surface-modified electrodes [40].

When AC impedance spectra are plotted in the form of Nyquist diagrams (Z_{im} as a function of Z_{re}, with frequency increasing from right to left), we can distinguish two regions typical of a reversible reaction at solid interface. At high frequencies the portion with semicircle shape corresponds to faradic electron-transfer at the electrodes, while at low frequencies curves give information about the diffusion process of transport of the redox species in the electrolyte to the electrode surface. Typical frequencies for diffusion are in the range of 1–10 Hz, while the electron transfer kinetics and double layer effects dominate at higher frequencies. Indeed the corresponding frequency range for most electrochemical reactions is from about 10 Hz to 10 kHz [41]. The time constant for double layer charging typically corresponds to a frequency region >10 kHz.

Useful information about what is going on at the electrode surface can be obtained by comparing the system with an equivalent circuit (Figure 1d). This is often a Randles circuit where the electron transfer resistance R_{et} accounting for the interfacial layer at the working electrode is kept in parallel with a capacitance C_{dl} (describing the electrical double layer at the interface), and a series Warburg impedance Z_w related to the depletion of the redox species at the interface. The additional series resistance R_s accounts for the uncompensated solution resistance. In the case of depressed semi-circles with the centre below the Z_{re} axis, the C_{dl} component in the equivalent circuit should be replaced with a constant phase element (CPE) which can be due to some electrode properties such as roughness [40]. This equivalent circuit can be simplified for the fit if diffusion process can be neglected. In general, R_{et} is very sensitive

to electrode modifications, so a progressive functionalization or biorecognition events at the electrodes surface can be easily detected.

The above mentioned potentiostat in combination with MULTI4 module and NOVA 1.10 software, allows the subsequential, automatic acquisition and recording of multi-electrodes measurements. As previously described, AC impedance spectra were recorded in a wide frequency range between 0.1 and 10^5 Hz and a Nyquist Plot was obtained in each condition under investigation. Following its validation in a research laboratory, the biochip can be connected to a portable impedance analyser as for example IVIUM pocketSTAT and connected to a laptop or to a mobile through an USB port, thus making a portable platform.

Each plotted curve comes from an average of at least five independent experiments (not the totality of experiments). Each biochip has been used for a single experiment.

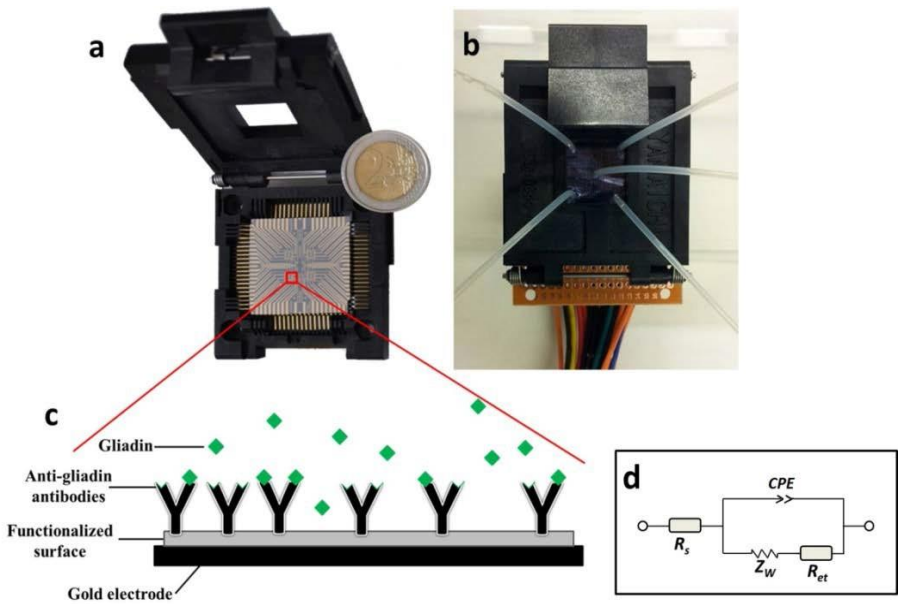

Figure 1. Setup of the gliadin-detection platform. **(a)** Gold microelectrode arrays fabricated on a silicon substrate and inserted in the measurement socket. **(b)** Final biochip with integrated microfluidic module which allows to deliver the sample solutions through the central or the peripheral holes to the **(c)** microelectrodes functionalized with specific antibodies. **(d)** Equivalent circuit for impedance spectroscopy transduction. The circuit includes ohmic resistance of the electrolyte solution R_s, Warburg impedance Z_w resulted from the ionic diffusion of the electrolyte, a constant phase element (CPE) and the electron transfer resistance R_{et}.

2.3 Sample preparation

To obtain a calibration curve, spiked samples with increasing concentrations of gliadin (from 0.5 µg/ml up to 200 µg/ml) in a solution of 60% ethanol in PBS were delivered to the sensing chambers through the central inlet hole of the microfluidic module (Figure 1b) and after 1 hour incubation, gliadin solution was replaced with the potassium hexacyanoferrate (II/III) redox solution. After calibration the biochip was employed to compare three types of beers of the same brand (gluten-free, lager and stout beer) for their gliadin content and three types of flours, also of the same brand (gluten-free, multi-cereals and wheat flour for semolina). The gluten-free beer employed here has the same ingredients of the lager beer (water, barley malt, rice, hops with a content of 5.4% ethanol for gluten-free and 4.6% for lager); stout beer contain only water, barley malt and hops with an alcoholic percentage of 6.6%. Flour samples have been selected among children nutrition products for weaning. Gluten-free flour contains corn (65%) and manihot (35%), multi-cereal flour contains wheat, rice, corn, barley and oat; semolina flour contains only wheat. We also used potatoes and rice flours (not containing gluten but prolamin-like proteins) as negative controls.

Beer samples were treated by adding ethanol to reach the 60% volume of the sample, and kept in agitation for 10 minutes. After waiting for 2 hours for the precipitation of ethanol insoluble components, the supernatant was collected to be analysed and delivered to the device sensing chambers (Figure 2a). Protocol for ethanolic extraction of gluten from flour samples (the same currently applied to obtain samples for ELISA tests [23, 42, 43]) requires 1 hour stirring of 250 mg flour in 10 ml of ethanol:water 60:40 at room temperature. After that mixed solution were centrifuged at 2500 rcf for 10 minutes and supernatant was removed for the analysis (Figure 2b). 90 µl were delivered into the biochips with a micropipette. This procedure was applied for all kinds of flours tested. Samples derived from both beer and flour extraction procedures were left into the device sensing chamber for 1 hour (Figure 2c). After that, samples were removed and

replaced with the above-mentioned redox couple solution. The same samples were used for mass spectrometry analysis.

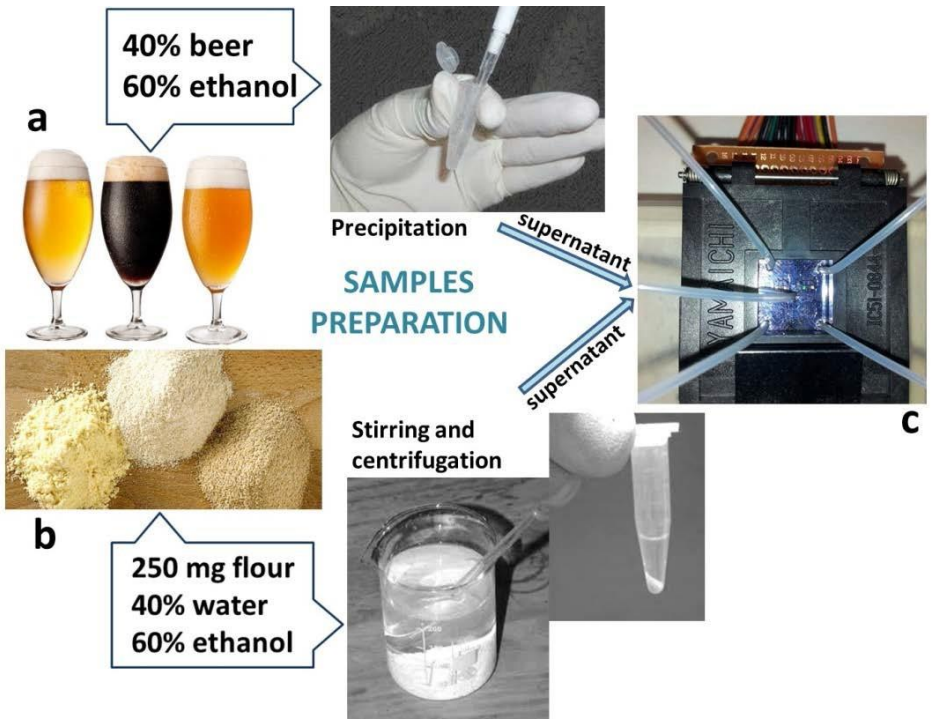

Figure 2. Preparation scheme for beer and flour samples. **(a)** Beers samples are prepared by simply adding ethanol to reach the 60% of the final volume. This causes the precipitation of ethanol-insoluble residues of beer and the solubilisation of gliadin. **(b)** Flours are dissolved in a solution of water and ethanol. After 1 hour stirring, the solution is centrifuged. Supernatants derived from beer or from flour samples are delivered to the inlet channel of the device **(c)** to perform analysis.

2.4 HPLC/ESI-MS analysis

The extracts were also analyzed by reverse-phase HPLC/ESI-MS employing a method from previously published reports [44-46] with a Thermo (Thermo Electron, USA) Deca XP Max ion trap mass spectrometer using electrospray ionization in the positive ion mode (ESI+). The HPLC instrument was a Thermo (Thermo Electron, USA) MS Pump equipped with a quaternary solvent delivery system, autosampler, and column heater and variable wavelength detector. Xcalibur software supplied by instrument manufacturer was used for instrument control and data analysis. In brief, 100 µl aliquots of each extract were filtered through a 0.45 µm membrane and separated on a 3.5 µm particle size and 300 Å pore size Waters Symmetry 300™ C4 2.1 X 150 mm reverse phase column with a flow rate was 0.25

ml/min. The column temperature was 50 °C and the eluent monitored at 210 nm. The mobile phases were A, 0.1 % formic acid (FA) in ultrapure water, and B, 0.1 % FA in acetonitrile. The eluting gradient (buffer B in A) was as follows: 24%B for 0.5 min, 24% B to 56% B in 45 min. After each run the column was cleaned with 90 % B (5 min) and equilibrated with 24% B for 5 min. The ES mass spectra were scanned from m/z 1000 to 4000, the source temperature was 275 °C. The cone voltage was 45 V. Quantitative analysis was performed by integration of the multiple charged ions assuming that the gliadin components have a similar tendency to ionize and using a gliadin standard from wheat (Sigma) for external calibration. The limit of quantification (LOQ) was defined as the sample whose analyte signal was at least 5 times the signal of a blank sample and the upper limit of quantification (ULOQ) was the highest calibration standard. Standard solutions with concentration ranges from 20 to 200 µg/ml (20, 40, 60, 100 and 200 µg/ml) of gliadin were prepared by diluting the 1 mg/ml stock solution. Experiments were performed in triplicate.

3. Results and discussion

3.1 Gliadin-immunochip calibration

The first step to quantify the gliadin concentration in a sample is to obtain a calibration curve. For this purpose, impedance spectra were acquired on functionalized devices using ethanolic solutions (60% ethanol in PBS) with known concentrations of gliadin. Once captured from the solution, by the antibodies immobilized on the electrode surface, antigens modulate the rate of electron transfer.

Quantitative values have been derived by modelling the charge flow by using a modified Randles circuit with a constant phase element and estimating the electron transfer resistance considering the equivalent circuit described in Figure 1d and neglecting diffusion in order to directly correlate R_{et} to the analyte concentration. Reproducible impedance values around 22 kΩ were recorded. Solutions with increasing concentrations (from 0.5 µg/ml up to 200 µg/ml) of gliadin were prepared and then incubated within the sensing chambers for 1h. R_{et} value ranging from around 24 kΩ, for the lowest concentration (0.5 µg/ml) up to around 262 kΩ for the highest one (200 µg/ml solution) were estimated from the Nyquist plots (Figure 3a) and a calibration curve (Figure 3b and inset) was obtained by plotting the electron transfer resistance R_{et} with its standard

deviation (SD) as a function of the gliadin concentration. From these recorded values we can establish that limit of quantification (LOQ) of our platform is of 0.5 µg/ml; calculated limit of detection (LOD) according to the method proposed by Armbuster and Pry in 2008 [47] (in which $LOD = LoB + 1.645x\ SD_{low\ concentration\ sample}$) is of 0.2 µg/ml of gliadin.

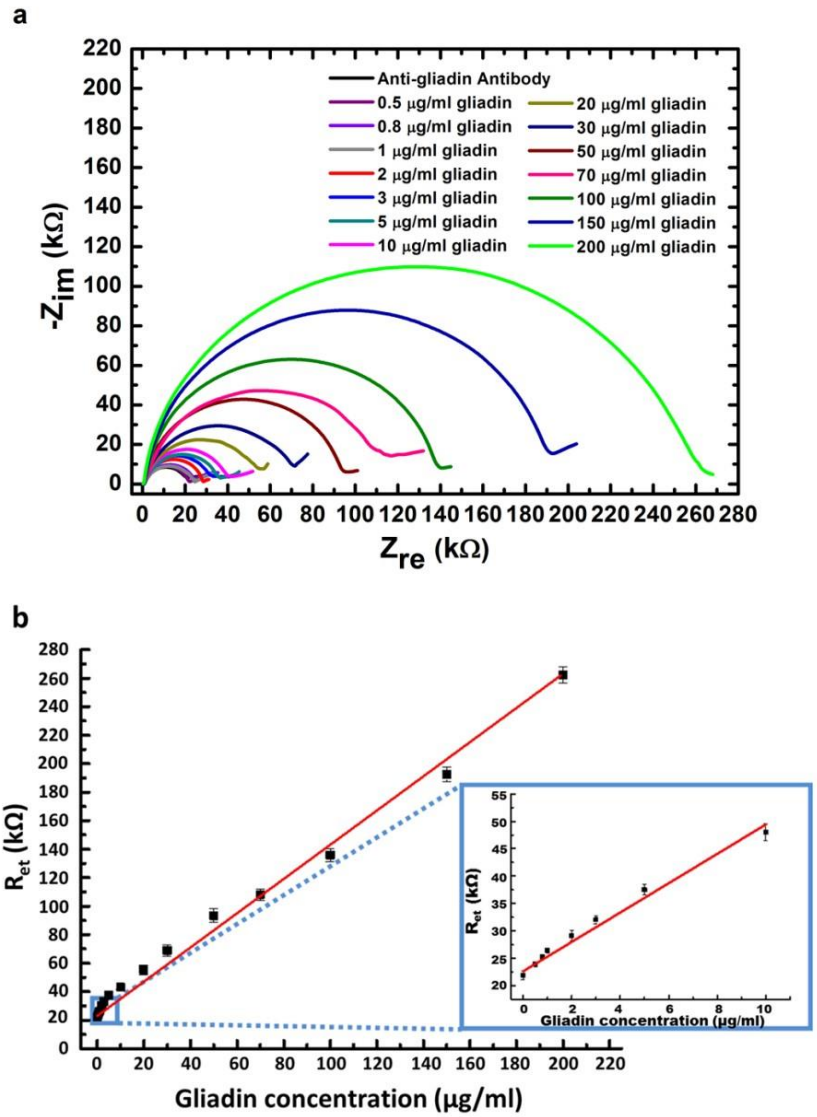

Figure 3. (a) Nyquist plots acquired during dose–response measurements and corresponding to the detection of different gliadin concentrations. **(b)** Calibration line in the range from 0.5 to 200 µg/ml gliadin concentration. **Inset:** for the 0-10 µg/ml gliadin concentration range.

3.2 On chip food analysis

Once calibrated, the gliadin immunochip was used to test its ability to analyse real samples from liquid and solid matrix. Cross contamination is a possibility that may happen if gluten-free and standar food is manufactured in the same place. To this regard we propose our platform as a powerful tool to check finished products before being sold. This is the reason why we selected products containing different gluten levels but having the same commercial brand. For example, three qualities of beer were considered: a gluten-free, a lager and a stout beer, containing an increasing content in gluten, due to a different amount and quality of cereals in their ingredients. Gluten levels in beer depend also on the brewing process of the raw materials. As a normal process gluten levels decrease due to precipitation during the mashing process, fermentation and beer stabilization. The final gluten content in beer has been approximately calculated as three orders of magnitude lower than in the raw malt [48]. Most of gluten-free beers are obtained with the same procedure as other qualities of beer and the elimination of gluten is often achieved as a last step by physical and chemical procedures, which anyway leave some amounts of gluten into the finished product.

As shown in the Nyquist plots in Figure 4a there is a sensible impedance increment between values associated to antibodies functionalization (black curve, $R_{et} \approx 21$ kΩ), to gluten-free beer green curve ($R_{et} \approx 29$ kΩ), and the other two blue and red curves associated to lager and stout beer with diameters of 60 kΩ and 81 kΩ respectively. This corresponds to a different amount in gliadin content in the three qualities of beer. Using the previously obtained calibration curve, we were able to establish a gliadin content of around 3 μg/ml in the ethanolic extract of gluten-free beer, 28 μg/ml in extract from lager beer and 48 μg/ml for stout beer.

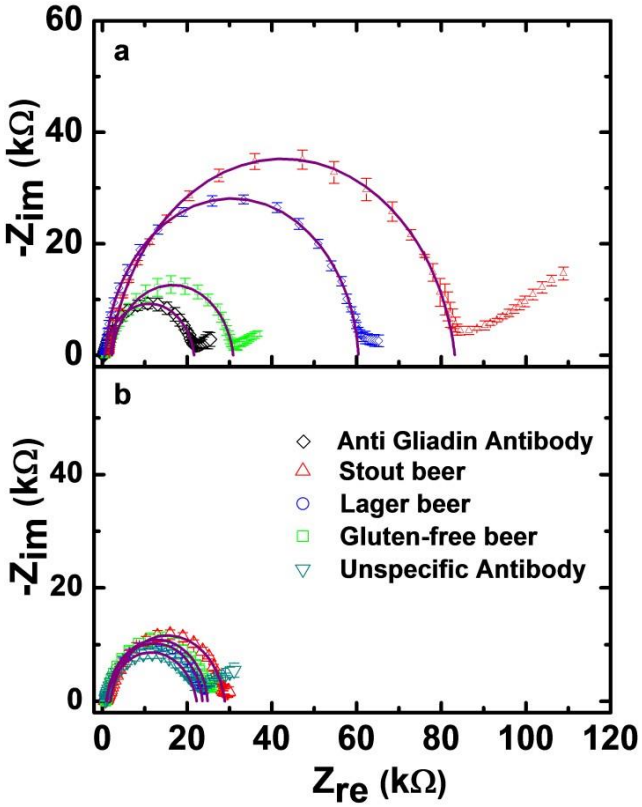

Figure 4. Nyquist plots for gliadin detection in beer samples and control experiments. Line curves over dotted Nyquist plots are the result of fitting. **(a)** Black line is related to antibody functionalization. Gluten-free beer results just in a small increase in impedance values (green curve); incubation with lager beer (blue curve) and stout beer (red curve) lead to still higher impedances accordingly to their sensitively larger gliadin content. **(b)** Negative control: Nyquist plots for the three beer qualities (same colour code) incubated on electrodes functionalized with unspecific antibodies (Anti-Listeria antibodies – dark cyan curve). A small increase in impedance is recorded for all the three samples in this case.

To evaluate any contribution from unspecific absorption of matrix components in our measurements, we set up a negative control placing a non-specific antibody in the functionalization procedure (Anti-Listeria antibody) and we tested all three types of beer (Figure 4b). In this control experiment an impedance value of 21 kΩ was recorded (dark cyan semicircle in Figure 4b), while for the three qualities of beer an increase of 2.5 kΩ (green line), 1 kΩ (blue line) and 6 kΩ (red line), respectively for gluten-free, lager and stout beer, above the baseline of the antibody was found. These data can be ascribed to a matrix effect due to unspecific binding of other components on the functionalized electrodes. In the case of gluten-free

beer, if we take into account the unspecific contribution (2.5 kΩ), the specific impedance increment above the antibody baseline is reduced to 4.5 kΩ, which accordingly to our calibration curve, it results in a gliadin concentration of 1.4 µg/ml in the ethanolic extract. As the extract was obtained in a 60% ethanolic solution we can estimate that gluten-free beer contains 3.5 µg/ml of gliadin, corresponding to about 7 µg/ml gluten, which is largely under the "gluten-free" threshold of 20 ppm. A similar calculation can be carried out also for the other two cases, which gives the values of 59 kΩ for the lager beer (corresponding to 25µg/ml gliadin in the extract and 62.5 µg/ml in beer), and 75 kΩ for stout (40 µg/ml gliadin content in the extract and 100 µg/ml in beer).

These results demonstrate the high degree of sensitivity and sensibility of our gliadin immunochip to determine the gliadin content of foodstuffs with a liquid matrix with. To test our device also with food samples derived from a solid matrix, we analysed three types of flours (from the same commercial brand) to be used in children nutrition and intended for children weaning. One of the three is a gluten-free flour made of corn and manihot, the second is a multi-cereal flour, and the third one is a wheat flour. The latter one has the highest gliadin content. Moreover we tested other two types of flours (rice and potatoes flours) in which there are some prolamin-like proteins. Flours have been processed with ethanolic extraction protocol for gliadin, as described in the Materials and Methods section; extracts were incubated for 1 hour into the chambers of the anti-gliadin functionalized devices and after that replaced with a redox couple solution to perform EIS measurements.

As shown in Figure 5a, samples derived of gluten-free flour (green curve) exhibit only a small increase in impedance values (6 kΩ) with respect to the baseline obtained with the anti-gliadin antibody alone (black plot,≈ 21 kΩ). Impedance curves corresponding to multi-cereal flour extracts have an electron transfer resistance of around 93 kΩ, while for wheat flour, impedance values reach a value of around 122 kΩ, which can be associated to a high amount of gliadin recognized by the anti-gliadin antibody layer deposited onto the electrode surface. To check the possibility of an unspecific absorption of flour

components above the active electrode surface, we set up again a negative control by depositing a layer of unspecific antibodies (Anti-Listeria antibody, dark cyan plot in Figure 5b) and incubating these devices with the same flour-extracts of the previous experiments. The unspecific impedance increase was found to be in a range from zero (red line related to wheat flour quite overlapping negative control line) to 7 kΩ (green line corresponding to gluten-free flour). As a consequence, the correction on the impedance values recorded with our anti-gliadin immunochip is small and can be taken into account by subtracting these values from the raw data. By interpolating the calibration curves, we estimated an amount of gliadin compatible with absence of gluten in gluten-free flour, around 55 µg/ml in multi-cereal flour and around 83 µg/ml in wheat flour.

Typically these data are reported as gliadin content per gram of solid product by assuming that all the gliadin amount in the processed flour was solubilized. Considering that we employed 250 mg of flour to prepare ethanolic solution to perform experiments, we can thus convert the amount of gliadin found in the extract in quantity of gliadin/ grams of former product. The conversion gives a quantity of gliadin of around 220 µg/g (440 µg/g of gluten content) in multicereal flour and 332 µg/g of gliadin in wheat flour with a total amount of gluten of 664 µg/g.

Finally, to test also the selectivity of our biochip for gliadin recognition, we tested two flours with zero gluten content (rice flour and potatoes flour) but containing prolamins-like proteins which belong to the same proteins family of gliadin. As shown from the graphs in Figure 5a only a small increase in impedance values is reported under the same experimental conditions. In particular light blue and pink curves (related respectively to potatoes and rice flour extracts) demonstrate a quite negligible impedance increment with respect to the baseline obtained from the anti-gliadin antibody (black curve around 21 k).

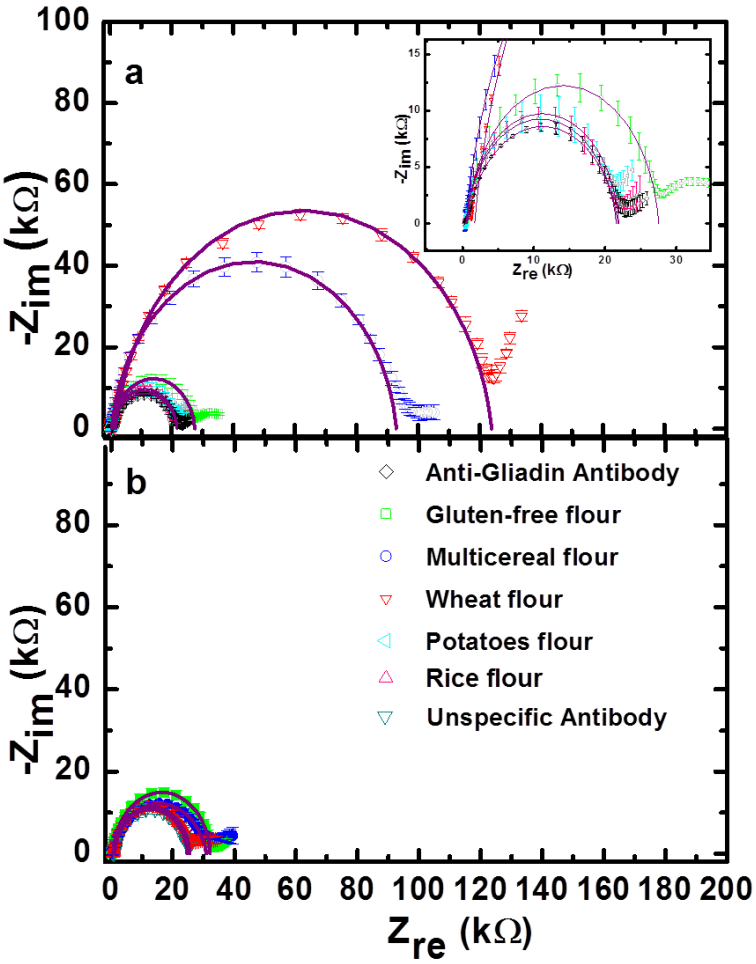

Figure 5. Nyquist plots for flour-derived samples on anti-gliadin functionalized electrodes and control. **(a)** Gluten-free flour (green curve) provides a slight increase in impedance values above the anti-gliadin antibody baseline (black curve); multi-cereal (blue curve) and wheat flour (red curve) samples elicit a large increase due to their high gliadin content. Only a slight impedance increase has been recorded over the antibody baseline for Nyquist plots of extracts of rice and potatoes flour (pink and light blue curves) as can be seen in the inset. **(b)** Negative control to evaluate matrix effects: incubation with the three types of flour-derived samples onto unspecific antibodies functionalization (Anti-Listeria antibodies) causes just a minor impedance increase with respect to the dark-cyan baseline.

3.3 Comparison with mass spectrometry analysis

The same extracts analysed by the proposed method based on EIS were also analysed by HPLC/ESI-MS to quantitate gliadins and compare the relevant results. It is interesting to note that a sample loop of 100 µl and formic acid as proton donor were necessary to get a LOQ in the low

ppm range. With formic acid instead of trifluoroacetic acid (TFA) in the eluent, despite the worse separation of gliadin fractions due to the lack of the ion pairing effect by TFA (not pertinent to our aims), a greater sensitivity of the MS detection and a LOQ of 20 µg/ml could be obtained. Table 1 lists the responses of both systems. Overall the methods gave results not statistically different and confirmed the suitability of the EIS device for gliadin analysis.

EXTRACTS FROM:	HPLC/ESI-MS	EIS measurement
Gluten-free beer	< LOQ	1.4 ± 0.5
Lager beer	23 ± 10	25 ± 2 µg/ml
Stout beer	34 ± 9	40 ± 2 µg/ml
Gluten-free flour	< LOQ	<0.5 µg/ml
Multicereal flour	65 ± 15	55±3 µg/ml
Wheat flour	98 ± 19	83 ±5 µg/ml

Table 1. Concentration of gliadins in sample extracts obtained by EIS sensor and HPLC/ESI-MS

4. Conclusion

Eating is not always a straight process. For CD patients, the ingestion of food containing gluten can lead to unpleasant consequences ranging from mild cutaneous rash to more severe allergic reactions with massive production of IgE against gliadin which represents the toxic portion in gluten. The only solution is a gluten-free diet, but this is a challenge for both food producer companies and CD patients, since great attention must be paid in everyday life and in production lines. Contaminations may occur every time both gluten-free and gluten containing foods are handled/manufactured together. The availability of portable and fast tools able to establish gliadin/gluten content from both liquid and solid matrices can strongly facilitate everyday life. Our gliadin immunochip provides a robust, fast and cheap platform for the quantification of gliadin concentration in commercial foodstuffs, as demonstrated here using beers and flours formulated for children nutrition and weaning, independently from their liquid or solid matrixes. Our results show that electrochemical impedance spectroscopy provides a simple and sensitive read-out thanks to the use of a redox couple to perform faradaic assays which are known to be typically

more sensitive than non-faradaic transduction because of the larger effect of antigen-antibody binding on the impedance real component than on the capacitive component [40]. Furthermore it is worth mentioning as the co-immobilization of BSA and the use of mixed self-assembled monolayers permit respectively to overcome potential problems related to the presence of unspecific interactions or the formation of pinholes in the molecular layer (which could allow the redox probe to penetrate close to the electrodes and exchange electrons with them) [40]. As a result, we reached a high degree of reproducibility and specificity, as demonstrated by the high number of negative controls performed to assess the ability of the platform in establishing threshold levels of gluten content in food and also in discriminating gliadin from other similar proteins, like prolamines from rice and potatoes. Moreover our results were also confirmed by standard techniques of ESI-Mass spectrometry and we demonstrated that our platform could reach best performances in terms of sensitivity with respect to that standard method. Notably we achieved a gliadin LOQ (0.5 μg/ml) that is 20 times lower than the worldwide threshold for gluten-free food, and even much better than the limits reached with currently employed ELISA-based methods operated in similar conditions. Thanks to compact dimensions and portability of our impedance-based immunoassay system, a strict contamination control of production chains in food industries which process both gluten-containing and gluten free products is even more realistic. These characteristics along with, fast response, cheapness and multiplexing possibility make the our biochip a robust and promising resource for food producers, CD affected people or for children with metabolic troubles.

5. References

[1] D.A. van Heel, J. West, Recent advances in coeliac disease, Gut, 55 (2006) 1037-1046.
[2] A. Alaedini, P.H.R. Green, Narrative Review: Celiac Disease: Understanding a Complex Autoimmune Disorder, Annals of Internal Medicine, 142 (2005) 289-298.
[3] C. Briani, D. Samaroo, A. Alaedini, Celiac disease: From gluten to autoimmunity, Autoimmunity Reviews, 7 (2008) 644-650.
[4] M. Hadjivassiliou, C.A. Williamson, N. Woodroofe, The immunology of gluten sensitivity: beyond the gut, Trends in Immunology, 25 (2004) 578-582.
[5] G.J. Tack, W.H.M. Verbeek, M.W.J. Schreurs, C.J.J. Mulder, The spectrum of celiac disease: epidemiology, clinical aspects and treatment, Nat. Rev. Gastroenterol. Hepatol., 7 (2010) 204-213.
[6] A. Fasano, I. Berti, T. Gerarduzzi, T. Not, R.B. Colletti, S. Drago, Y. Elitsur, P.H. Green, S. Guandalini, I.D. Hill, M. Pietzak, A. Ventura, M. Thorpe, D. Kryszak, F. Fornaroli, S.S. Wasserman, J.A. Murray, K. Horvath, Prevalence of celiac disease in at-risk and not-at-risk groups in the United States: a large multicenter study, Arch Intern Med, 163 (2003) 286-292.
[7] J.Y. Kang, A.H.Y. Kang, A. Green, K.A. Gwee, K.Y. Ho, Systematic review: worldwide variation in the frequency of coeliac disease and changes over time, Alimentary Pharmacology & Therapeutics, 38 (2013) 226-245.
[8] F. Biagi, G.R. Corazza, Clinical features of coeliac disease, Digestive and Liver Disease, 34 (2002) 225-228.
[9] M. Rashid, M. Zarkadas, A. Anca, H. Limeback, Oral Manifestations of Celiac Disease: A Clinical Guide for Dentists, J. Can. Dent. Assoc., 77 (2011).
[10] U. Volta, V. Villanacci, Celiac disease: diagnostic criteria in progress, Cell. Mol. Immunol., 8 (2011) 96-102.
[11] www.fda.gov/downloads/Food/GuidanceRegulation/UCM205938.ppt+&cd=1&hl=it&ct=clnk&gl=it

[12] C. Catassi, E. Fabiani, G. Iacono, C. D'Agate, R. Francavilla, F. Biagi, U. Volta, S. Accomando, A. Picarelli, I. De Vitis, G. Pianelli, R. Gesuita, F. Carle, A. Mandolesi, I. Bearzi, A. Fasano, A prospective, double-blind, placebo-controlled trial to establish a safe gluten threshold for patients with celiac disease, The American Journal of Clinical Nutrition, 85 (2007) 160-166.
[13] T. Thompson, E. Mendez, Commercial assays to assess gluten content of gluten-free foods: why they are not created equal, J Am Diet Assoc, 108 (2008) 1682-1687.
[14] JOINT FAO/WHO FOOD STANDARDS PROGRAMME CODEX ALIMENTARIUS COMMISSION Thirty first Session Geneva, Switzerland, 30 June - 5 July 2008
[15] P. Ferranti, G.R. Marnone, G. Picariello, F. Addeo, Mass spectrometry analysis of gliadins in celiac disease, J. Mass Spectrom., 42 (2007) 1531-1548.
[16] H. Wieser, Chemistry of gluten proteins, Food Microbiology, 24 (2007) 115-119.
[17] R. Haraszi, H. Chassaigne, A. Maquet, F. Ulberth, Analytical methods for detection of gluten in food--method developments in support of food labeling legislation, J AOAC Int, 94 (2011) 1006-1025.
[18] http://www.miobs.com/english/product/food_allergen_elisa_kits/dl/gdrev1.pdf
[19] B. Morón, Á. Cebolla, H. Manyani, M. Álvarez-Maqueda, M. Megías, M.d.C. Thomas, M.C. López, C. Sousa, Sensitive detection of cereal fractions that are toxic to celiac disease patients by using monoclonal antibodies to a main immunogenic wheat peptide, The American Journal of Clinical Nutrition, 87 (2008) 405-414.
[20] S. Haas-Lauterbach, U. Immer, M. Richter, P. Koehler, Gluten fragment detection with a competitive ELISA, J AOAC Int, 95 (2012) 377-381.
[21] J.R. Mujico, M. Lombardía, M.C. Mena, E. Méndez, J.P. Albar, A highly sensitive real-time PCR system for quantification of wheat contamination in gluten-free food for celiac patients, Food Chemistry, 128 (2011) 795-801.
[22] A.M. Peres, L.G. Dias, A.C.A. Veloso, S.G. Meirinho, J.S. Morais, A.A.S.C. Machado, An electronic tongue for gliadins semi-quantitative detection in foodstuffs, Talanta, 83 (2011) 857-864.
[23] P.-T. Chu, C.-S. Lin, W.-J. Chen, C.-F. Chen, H.-W. Wen, Detection of Gliadin in Foods Using a Quartz Crystal Microbalance Biosensor That Incorporates Gold Nanoparticles, Journal of Agricultural and Food Chemistry, 60 (2012) 6483-6492.
[24] C.M. Lo, C.R. Keese, I. Giaever, Impedance analysis of MDCK cells measured by electric cell-substrate impedance sensing, Biophysical Journal, 69 (1995) 2800-2807.
[25] J. Wegener, C.R. Keese, I. Giaever, Electric cell-substrate impedance sensing (ECIS) as a noninvasive means to monitor the kinetics of cell spreading to artificial surfaces, Experimental Cell Research, 259 (2000) 158-166.
[26] I. Giaever, C.R. Keese, Monitoring fibroblast behavior in tissue culture with an applied electric field, Proceedings of the National Academy of Sciences of the United States of America, 81 (1984) 3761-3764.
[27] E. Primiceri, M.S. Chiriaco, R. Rinaldi, G. Maruccio, Cell chips as new tools for cell biology - results, perspectives and opportunities, Lab on a Chip, 13 (2013) 3789-3802.
[28] G.H. Hui, S.S. Mi, Q.Q. Chen, X. Chen, Sweet and bitter tastant discrimination from complex chemical mixtures using taste cell-based sensor, Sens. Actuator B-Chem., 192 (2014) 361-368.
[29] T.M. Curtis, M.W. Widder, L.M. Brennan, S.J. Schwager, W.H. van der Schalie, J. Fey, N. Salazar, A portable cell-based impedance sensor for toxicity testing of drinking water, Lab on a Chip, 9 (2009) 2176-2183.
[30] H.Y. Yin, F.L. Wang, A.L. Wang, J. Cheng, Y.X. Zhou, Bioelectrical impedance assay to monitor changes in aspirin-treated human colon cancer HT-29 cell shape during apoptosis, Analytical Letters, 40 (2007) 85-94.
[31] J.Y. Park, S.M. Park, DNA Hybridization Sensors Based on Electrochemical Impedance Spectroscopy as a Detection Tool, Sensors, 9 (2009) 9513-9532.
[32] Z.W. Zou, J.H. Kai, M.J. Rust, J. Han, C.H. Ahn, Functionalized nano interdigitated electrodes arrays on polymer with integrated microfluidics for direct bio-affinity sensing using impedimetric measurement, Sensors and Actuators a-Physical, 136 (2007) 518-526.
[33] M.S. Chiriaco, E. Primiceri, A. Montanaro, F. de Feo, L. Leone, R. Rinaldi, G. Maruccio, On-chip screening for prostate cancer: an EIS microfluidic platform for contemporary detection of free and total PSA, Analyst, 138 (2013) 5404-5410.
[34] M.S. Chiriaco, E. Primiceri, A.G. Monteduro, A. Bove, S. Leporatti, M. Capello, S. Ferri-Borgogno, R. Rinaldi, F. Novelli, G. Maruccio, Towards pancreatic cancer diagnosis using EIS biochips, Lab Chip, 13 (2013) 730-734.
[35] T. Mairal, I. Frese, E. Llaudet, C.B. Redondo, I. Katakis, F. von Germar, K. Drese, C.K.O. Sullivan, Microfluorimeter with disposable polymer chip for detection of coeliac disease toxic gliadin, Lab on a Chip, 9 (2009) 3535-3542.
[36] Y.S. Fung, Y.Y. Wong, Self-assembled monolayers as the coating in a quartz piezoelectric crystal immunosensor to detect salmonella in aqueous solution, Anal. Chem., 73 (2001) 5302-5309.
[37] F. Xiao, N. Zhang, H. Gu, M. Qian, J. Bai, W. Zhang, L. Jin, A monoclonal antibody-based immunosensor for detection of Sudan I using electrochemical impedance spectroscopy, Talanta, 84 (2011) 204-211.
[38] W.T. Kim, T.W. Okita, STRUCTURE, EXPRESSION, AND HETEROGENEITY OF THE RICE SEED PROLAMINES, Plant Physiol., 88 (1988) 649-655.
[39] A.C. Kapoor, S.L. Desborough, P.H. Li, Potato tuber proteins and their nutritional quality, Potato Res, 18 (1975) 469-478.
[40] E. Katz, I. Willner, Probing Biomolecular Interactions at Conductive and Semiconductive Surfaces by Impedance Spectroscopy: Routes to Impedimetric Immunosensors, DNA-Sensors, and Enzyme Biosensors, Electroanalysis, 15 (2003) 913-947.
[41] L. Yang, Y. Li, AFM and impedance spectroscopy characterization of the immobilization of antibodies on indium-tin oxide electrode through self-assembled monolayer of epoxysilane and their capture of Escherichia coli O157:H7, Biosensors and Bioelectronics, 20 (2005) 1407-1416.
[42] B. Moron, A. Cebolla, H. Manyani, M. Alvarez-Maqueda, M. Megias, M.D.C. Thomas, M.C. Lopez, C. Sousa, Sensitive detection of cereal fractions that are toxic to celiac disease patients by using monoclonal antibodies to a main immunogenic wheat peptide, Am. J. Clin. Nutr., 87 (2008) 405-414.
[43] M.C. Mena, M. Lombardía, A. Hernando, E. Méndez, J.P. Albar, Comprehensive analysis of gluten in processed foods using a new extraction method and a competitive ELISA based on the R5 antibody, Talanta, 91 (2012) 33-40.
[44] H. Wieser, Comparative investigations of gluten proteins from different wheat species I. Qualitative and quantitative composition of gluten protein types, Eur Food Res Technol, 211 (2000) 262-268.
[45] G. Mamone, P. Ferranti, L. Chianese, L. Scafuri, F. Addeo, Qualitative and quantitative analysis of wheat gluten proteins by liquid chromatography and electrospray mass spectrometry, Rapid communications in mass spectrometry : RCM, 14 (2000) 897-904.
[46] B. Lagrain, M. Brunnbauer, I. Rombouts, P. Koehler, Identification of Intact High Molecular Weight Glutenin Subunits from the Wheat Proteome Using Combined Liquid Chromatography-Electrospray Ionization Mass Spectrometry, PLoS One, 8 (2013) e58682.
[47] D.A. Armbruster, T. Pry, Limit of Blank, Limit of Detection and Limit of Quantitation, The Clinical Biochemist Reviews, 29 (2008) S49-S52.
[48] P. Dostalek, I. Hochel, E. Mendez, A. Hernando, D. Gabrovska, Immunochemical determination of gluten in malts and beers, Food Addit Contam, 23 (2006) 1074-1078.